Coating flow of viscous Newtonian liquids on a rotating vertical disk

Nilesh H. Parmar,[1] Mahesh S. Tirumkudulu,[1] and E. J. Hinch[2]
[1]*Department of Chemical Engineering, Indian Institute of Technology-Bombay, Powai, Mumbai 400076, India*
[2]*Department of Applied Mathematics and Theoretical Physics, Centre for Mathematical Sciences, University of Cambridge, Wilberforce Road, Cambridge CB3 0WA, United Kingdom*

(Received 31 March 2009; accepted 10 September 2009; published online 22 October 2009)

We study a Newtonian viscous liquid coating a vertical rotating disk in the creeping flow regime. Experiments were performed at varying disk rotation speeds and liquid volumes, and the thickness profile at steady state was measured. While the maximum liquid supported by the rotating disk varied with rotation rate and liquid viscosity, the numerical value of a dimensionless number signifying the ratio of gravity to viscous forces was the same in all the cases, $\gamma=0.30$. A lubrication analysis for the time evolution of the film thickness that accounted for gravity, surface tension, and viscous forces was solved numerically to steady state. The predicted thickness profiles are in quantitative agreement with those obtained experimentally. The lubrication equation at steady state was solved analytically in the absence of surface tension to obtain constant height contours that were circular and symmetric about the horizontal axis. However to obtain a complete solution, knowledge of the height variation across the contours is required, and this is controlled by the surface tension. On including this effect, we derived an asymptotic solution to predict thickness profiles that agree well with measurements for large values of viscosity or rotation rates. © *2009 American Institute of Physics*. [doi:10.1063/1.3250858]

I. INTRODUCTION

Thin film flows are encountered in a variety of settings such as spreading of paints, coatings and adhesives on substrates, gravity currents under water, lava flows, and linings of mammalian lungs. They also appear in various modern technological applications such as microchip production and microfluidic devices. The review of Oron *et al.*[1] describes thin film flows that include effects of viscous, surface tension and body forces, thermocapillarity, evaporation, and van der Waals attraction.

It is well known that when a vertical plate is withdrawn from a pool of viscous liquid, the final thickness of the liquid film carried by the plate is determined from the competition between the viscous force that carries the liquid upward against drainage caused by gravity.[2] Alternatively, it is also possible to support liquid on a finite sized vertical plate by rotating the plate about its horizontal axis. For a stationary vertical surface, a film of liquid of thickness h drips off under gravity with a velocity that scales as $\rho g h^2/\mu$. Here, g is the gravitational acceleration, h is the film thickness and, μ and ρ are the liquid viscosity and density, respectively. Thus the thickness that can be supported by a rotating disk without the liquid dripping is obtained by equating this velocity with the rotational velocity of the disk ΩR, $h \sim \sqrt{\mu \Omega R/\rho g}$. It then follows that the total volume of liquid that a rotating disk can support is proportional to $\sqrt{\mu \Omega R^5/\rho g}$. However, the thickness profile across the plate is strictly determined by a balance of gravity, viscous, and surface tension forces. A related one-dimensional analog is that studied by Moffatt[3] who investigated thin viscous films on the outer surface of a horizontal rotating cylinder using a lubrication approximation. Our goal here is to investigate the two-dimensional problem of the flow of viscous Newtonian liquids coated on a vertical rotating disk via experiments, numerical simulations, and asymptotic analysis.

A variation of the rotating vertical disk geometry that is important industrially is a rotating disk reactor (RDR), which consists of a stainless steel disk mounted on a horizontal shaft accommodated in a cylindrical shell partially filled with liquid.[4] The rotating disk carries a thin film of liquid, which is brought in contact with a gas phase for enhanced gas-liquid mass transfer. The main advantage of the RDR is that the interfacial gas-liquid area is constant and known. Further, the reactor is known to give higher performance at the expense of less energy in comparison with other conventional methods.[5] The RDR finds extensive industrial applications such as in photocatalytic degradation of chlorinated phenols and chlorinated aromatics,[6] in citric acid production by aerobic fermentation using a bacterial culture[7] and in the production of thermoplastic polymer such as polycarbonates.[8] In spite of the several industrial applications of the thin film flow on a rotating vertical disk, it has not received much attention in literature while the related case of spin coating, wherein a thin film of liquid spreads over a rotating horizontal substrate by the action of centrifugal force, has been well studied.[9–12] In spin coating, gravity acts perpendicular to the plane of the substrate, leading to an axisymmetric film that spreads radially outward. In contrast, gravity acts parallel to the disk surface in our case leading to a nonaxisymmetric film.

We first report experimental measurements of the thickness profile for varying liquid volumes, rotation rates, and liquid viscosities on slowly rotating vertical disks. Since moving contact lines are difficult to analyze, the contact line

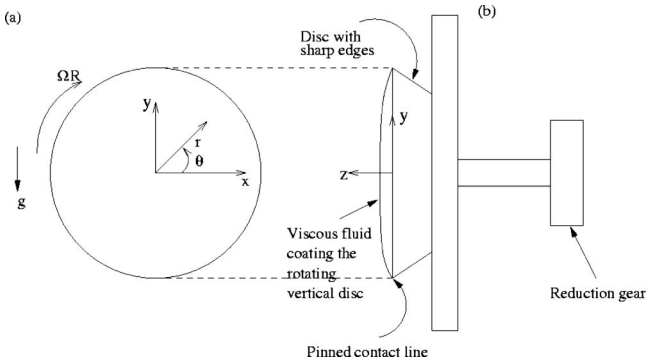

FIG. 1. Schematic of the experimental setup. (a) Front view of the rotating disk; (b) side view.

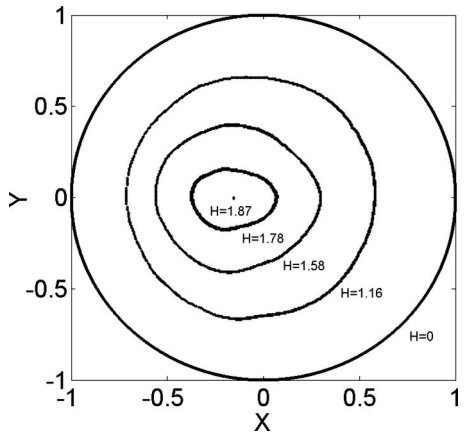

FIG. 2. Contours of constant height on a 7 cm diameter circular disk rotating clockwise at 2 rpm coated with 5 ml of silicone oil of viscosity 35 Pa s. The x and y coordinates are nondimensionalized by the disk radius while the thickness is rendered dimensionless by the average film thickness.

was pinned at the periphery of the disk in all experiments. Next, a lubrication analysis for the thin film results in a time evolution equation for the film thickness. The equation was solved numerically using a time marching finite difference scheme to obtain the steady state solution. The numerical profiles are in close quantitative agreement with the experiments even for low rotation rates or large volumes when the lubrication approximation may not be valid. A better physical insight into the nature of the flow is obtained from an analytical solution of the lubrication equation, which predicts circular height contours in the absence of surface tension. Interestingly, the centers of the contours are offset from the axis of the disk on the horizontal diameter. It is next shown that it is necessary to include surface tension in order to capture the thickness variation across the contours. We demonstrate this by an asymptotic solution which predicts thickness profiles that agree well with measurements for large values of viscosity or rotation rates.

II. EXPERIMENTS

Figure 1 presents a schematic of the experimental setup. A vertical flat stainless steel disk was attached to a stepper motor via a 1:5 reduction pulley so that the disk could be rotated over a wide range of rotation rates. Liquid volumes were selected so that the liquid coated the disk completely with the contact line pinned at the circumference of the disk. The latter was ensured by fabricating disks with sharp edges. The thickness profile of the film at steady state was measured accurately using an xyz-micrometer traverse of least count of 0.01 mm. This in turn was placed on an xy-traverse with a coarse movement of 100 mm in each direction and a least count of 1 mm. A needle was attached to the xyz-traverse to probe the entire surface of disk.

Since the accuracy of the final measurement depends on the alignment of the traverse with respect to the vertical disk, a detailed calibration was performed prior to the experiments. At a fixed y, the needle was made to contact the disk surface at a number of points along the x direction (Fig. 1). This was repeated at various vertical positions (for different y) on the disk surface. The maximum variation in the disk position over the entire surface was found to be less than ± 0.05 mm. Once the average disk surface position (z coordinate of the disk surface) was known, the liquid film thickness profile was determined by noting the z coordinate of the liquid film (the free surface) at various locations on the disk and then subtracting the disk surface position from it.

Experiments were performed with transparent Newtonian silicon oils with viscosities of 5 and 35 Pa s, density of 900 kg/m^3, and surface tension of 31 mN/m, at varying rotation speeds, disk diameters, and liquid volumes. Each experiment involved injecting a fixed quantity of oil onto the disk so that the liquid coated the entire disk. The volumes chosen for the experiments were such that the film thickness over most of the disk surface was much greater than the error in measurement. For all the experiments, the film thickness was measured at steady state at more than 60 points on the disk surface and interpolated using MATLAB© to obtain the full thickness profile. The steady state was said to be achieved when the thickness profile measured at different times was identical. The thickness data points were integrated over the whole domain to determine the total volume of liquid. In all experiments, the numerically determined liquid volume differed little (3% error) from the amount actually injected, thereby confirming the accuracy of the measurement system.

III. EXPERIMENTAL RESULTS

Figure 2 shows the contours of the film thickness obtained from the interpolated values for an experiment performed on a 7 cm diameter disk rotating at 2 rpm, coated with 5 ml of silicone oil of viscosity 35 Pa s. The film thickness has been normalized by its average value h_0, i.e. we plot $H=h/h_0$. The height contours appear to be fairly symmetric about the horizontal diameter with larger thicknesses on the upward moving left half of the disk. In fact, the point of maximum height ($H=1.87$) occurs along the horizontal diameter on the left half of the disk. This is because the liquid velocities are lower for $x<0$ compared to $x>0$, where both gravity and viscous forces act in the same direction. Thus for the same volume flux, we would expect thicker films for $x<0$.

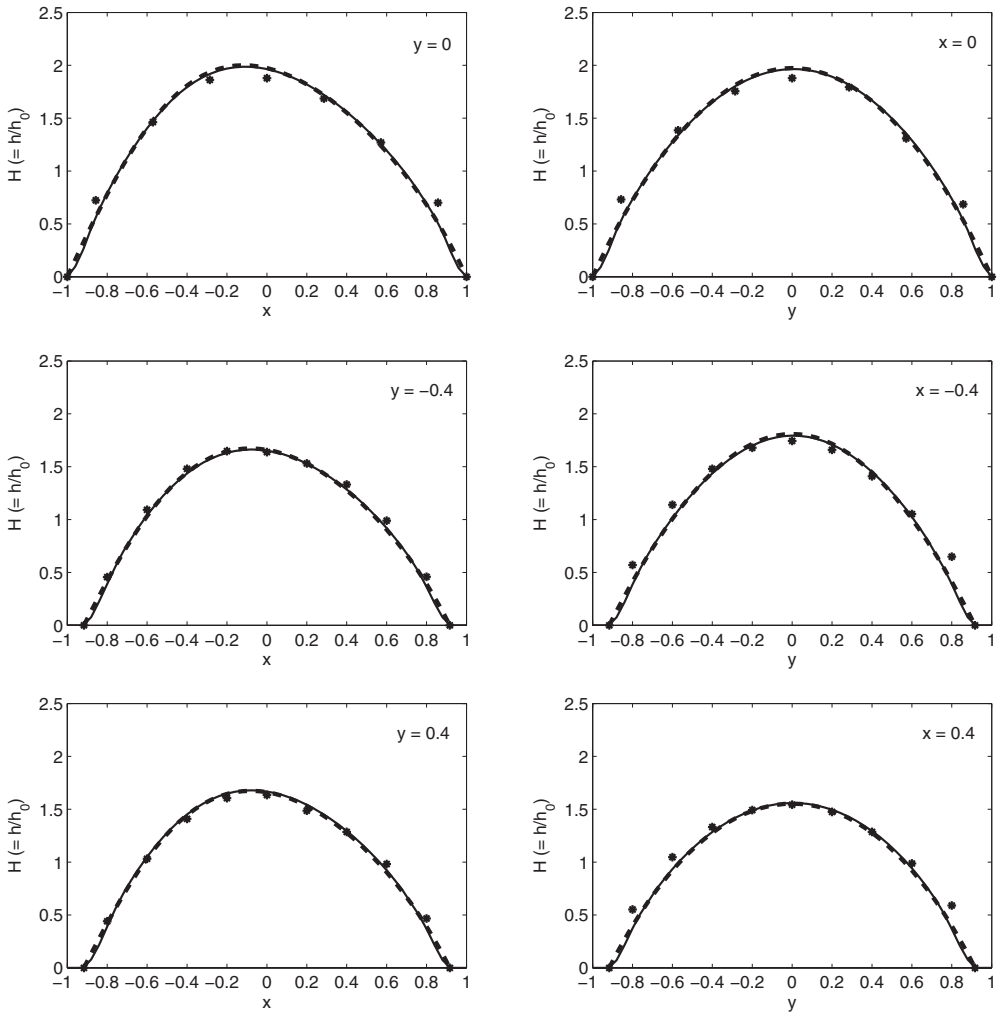

FIG. 3. Comparison of experiments (●), numerical results (solid line), asymptotic solution (dashed line) along different constant x- and constant y-lines, for a rotation rate of 4 rpm, liquid volume of 5 ml, and $\mu=35$ Pa s on a 7 cm diameter disk. Hence the thinness of the film is $h_0/R=0.037$, the strength of gravity $\gamma=0.029$, and the strength of surface tension $\alpha=3.1\times10^{-6}$.

The thickness measurements are plotted in Figs. 3–5 along three vertical and horizontal sections. The maximum error in the measurement was less than 5% of the average film thickness. With decreasing rotation rate at a fixed volume, the left-right asymmetry increases, implying that more liquid is accumulated in $x<0$. Interestingly, the profiles along the vertical section appear more or less symmetric even though one would have expected the downward pull of gravity to have accumulated a greater amount of liquid at the bottom of the disk.

We also determined the maximum supportable liquid volume on disks with diameters of 7 and 8 cm at rotation rates of 1–5 rpm and for silicon oils of viscosities of 5 and 35 Pa s. Recall that the preliminary scaling showed the thickness should scale as $h\sim\sqrt{\mu R\Omega/\rho g}$. We therefore plot $\gamma=\rho g h_0^2/\mu\Omega R$ at the maximum supportable volume against the rotation rate for the two viscosities. We find that the value of $\gamma_{\max}$ is constant and approximately equal to 0.30 for all the experiments, see Fig. 6. In other words, the maximum supported volume is $V_{\max}\approx 1.72\sqrt{\mu\Omega R^5/\rho g}$. This is reminiscent of a similar result obtained for the flow of viscous liquid coating the outside surface of a rotating cylinder[3] where the maximum supported volume is $4.44\sqrt{\mu\Omega R^5/\rho g}$ per unit length of the cylinder. To better appreciate these observations, we develop a lubrication approximation to predict the film thickness profile for a viscous liquid coating a vertical rotating disk.

IV. LUBRICATION MODEL

We use the standard lubrication approximation for the flow of a thin film of viscous liquid. Inertial effects are ignored. The local thickness of the film on the disk $h(x,y,t)$ changes in time due to a divergence in a flux of liquid $\mathbf{q}$ in the xy-plane,

$$\frac{\partial h}{\partial t}+\nabla\cdot\mathbf{q}=0.$$

The flux has contributions from the moving surface of the disk, gravity, and a pressure gradient,

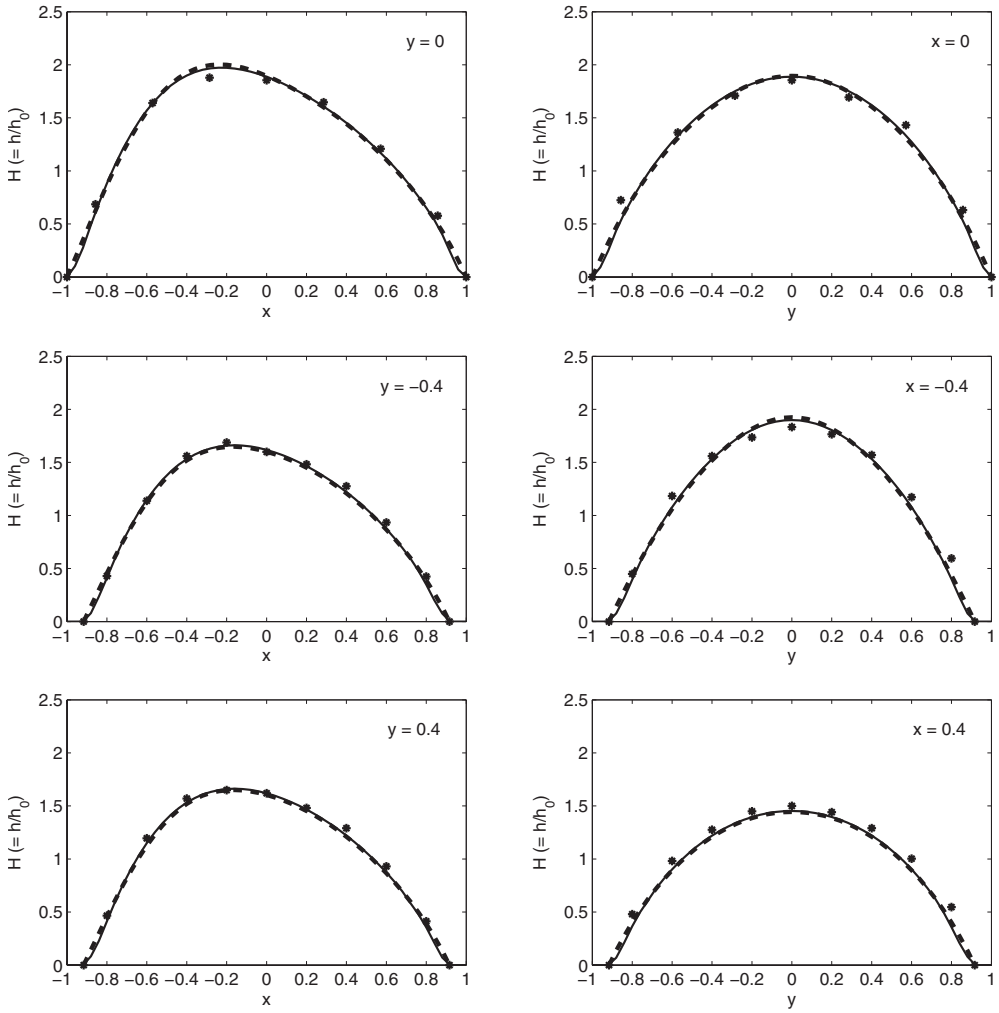

FIG. 4. Comparison of experiments (●), numerical results (solid line), asymptotic solution (dashed line) along different constant x- and constant y-lines, for a rotation rate of 2 rpm, liquid volume of 5 ml, and $\mu=35$ Pa s on a 7 cm diameter disk. Hence the thinness of the film is $h_0/R=0.037$, the strength of gravity $\gamma=0.058$, and the strength of surface tension $\alpha=6.2\times10^{-6}$.

$$\mathbf{q}=\mathbf{\Omega}\wedge\mathbf{x}h+\frac{\rho h^3}{3\mu}\mathbf{g}-\frac{h^3}{3\mu}\boldsymbol{\nabla}p,$$

where the pressure p is the capillary pressure due to the curvature κ of the free surface,

$$p=-\sigma\kappa=-\sigma\boldsymbol{\nabla}^2h.$$

Here $\mathbf{\Omega}$ is the angular velocity of the disk, ρ is the density of the fluid, μ is its viscosity, $\mathbf{g}$ is the gravitational acceleration, and σ is the surface tension.

We nondimensionalize the problem by scaling the position on the disk x and y by the radius of the disk R, the film thickness by its average value h_0 $(=V/\pi R^2$, where V is the volume of the film), and time by the rotation rate Ω. There are then three nondimensional groups: The thinness of the film h_0/R which we assume is small in making the lubrication approximation and is around 0.04 in the experiments, the strength of the effect of gravity,

$$\gamma=\frac{\rho g h_0^2}{\mu\Omega R},$$

and the strength of the effect of surface tension,

$$\alpha=\frac{\sigma h_o^3}{\mu\Omega R^4}.$$

As we noted in the introduction, the strength of gravity γ cannot be large if the disk is to rotate faster than the film wishes to drip off the disk. The strength of surface tension is typically quite small, around 10^{-5}.

The nondimensionalized governing equation is then

$$\frac{\partial h}{\partial t}+\boldsymbol{\nabla}\cdot\left(\mathbf{\Omega}\wedge\mathbf{x}h+\frac{1}{3}\gamma h^3\mathbf{g}+\frac{1}{3}\alpha h^3\boldsymbol{\nabla}\kappa\right)=0, \tag{1}$$

where $\mathbf{\Omega}$ and $\mathbf{g}$ are now unit vectors. For boundary conditions, we assume that the film is pinned on the circumference of the disk and that the radial component of the flux vanishes there,

$$h=0 \quad \text{and} \quad q_r=0 \quad \text{at} \quad r=1.$$

The latter requires the curvature not to be singular. The volume normalization is

$$\int_{r\le1}h\,dA=\pi.$$

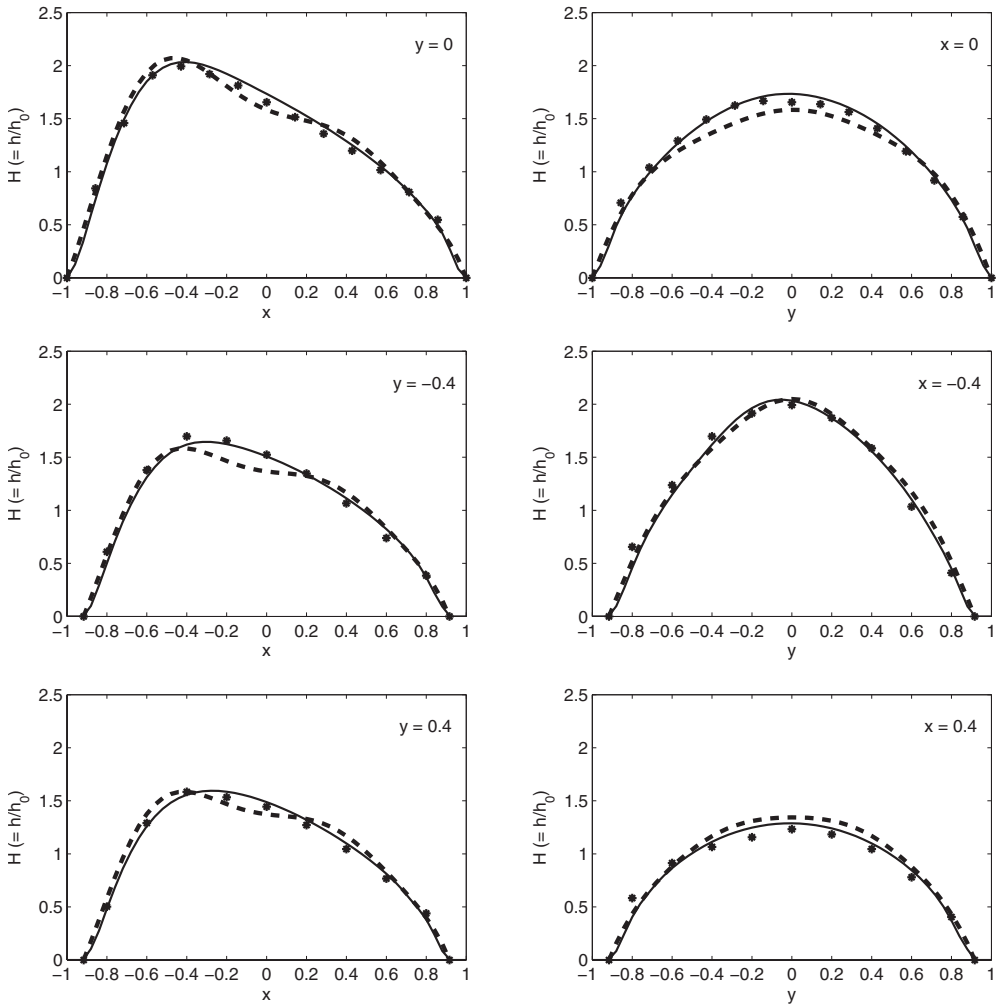

FIG. 5. Comparison of experiments (●), numerical results (solid line), asymptotic solution (dashed line) along different constant x- and constant y-lines, for a rotation rate of 1 rpm, liquid volume of 5 ml, and $\mu=35$ Pa s on a 7 cm diameter disk. Hence the thinness of the film is $h_0/R=0.037$, the strength of gravity $\gamma=0.116$, and the strength of surface tension $\alpha=1.2\times10^{-5}$.

V. NUMERICAL SOLUTION

The governing Eq. (1) was discretized in Cartesian coordinates over the square domain $-1\leq x,y\leq 1$. This avoided the coordinate singularity of polar coordinates. We used finite differences with second-order central differencing in space and first-order explicit differencing in time. The boundary condition was enforced by requiring the film thickness to vanish at all points on or beyond the circular boundary of the disk,

$$h=0 \quad \text{for} \quad r\geq 1.$$

The initial condition was taken to be a spherical cap of the required volume. The governing equation was then integrated forward in time until a steady state was achieved. Simulations were performed for varying grid spacing and time steps to check the accuracy. Typical grids of 100×100 were required with time steps less than 0.1. For large values of the strength of gravity γ, the spatial resolution had to be increased in order to conserve the volume of the film, e.g., for $\gamma=0.16$ a resolution of 150×150 was needed. For this reason we restricted computations to $\gamma\leq0.12$.

The profiles of the film thickness obtained numerically are compared to the experimental profiles in Figs. 3–5, where the solid curves are the numerical results and the experimental results the points. There is quantitative agreement. The plots for $y=0$ show more liquid on the upward moving left

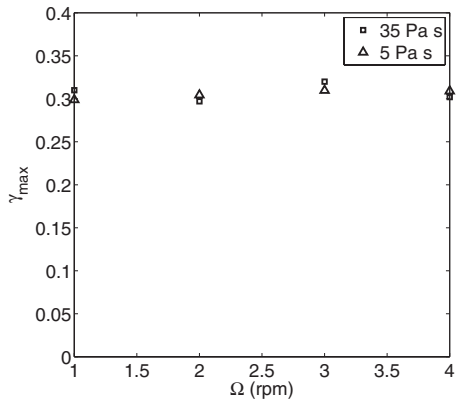

FIG. 6. Values of the strength of gravity $\gamma_{\max}$ for a maximum possible liquid volume supported by a rotating disk of diameter 7 cm as a function of rotation rate for two different viscosity liquids.

half of the disk, where the viscous and gravity forces oppose one another. The location of maximum thickness moves away from the center of the disk as the strength of gravity γ increases. The plots for $x=0$ are symmetric about the horizontal axis $y=0$, except perhaps for the highest $\gamma=0.116$ in Fig. 5.

VI. STEADY STATE AT ZERO SURFACE TENSION

The strength α of the surface tension is small, around 10^{-5}, so we start by setting the term to zero. The governing Eq. (1) then becomes, for the steady state,

$$(\mathbf{\Omega} \wedge \mathbf{x} + \gamma h^2 \mathbf{g}) \cdot \nabla h = 0. \tag{2}$$

Thus the thickness of the film h is constant around a circle,

$$|\mathbf{x} - \gamma h^2 \mathbf{\Omega} \wedge \mathbf{g}| = \text{const}. \tag{3}$$

It should be noted that the circles are characteristics of the hyperbolic Eq. (2) and are not current lines of the flux $\mathbf{q}$ nor streamlines of the fluid at any level within the film.

The centers of the circular characteristics are offset from the center of the disk by γh^2 horizontally on the upward moving side of the disk; the greater the thickness h, the greater the offset. This behavior is the same as that observed experimentally in Fig. 2.

While Eq. (2), with zero surface tension, gives h constant around the circular characteristics, it does not give the variation across the different circles. Surface tension, however small, must be taken into account to determine the variation across the circles. Now with zero gravity $\gamma=0$, surface tension makes the film into a spherical cap, which in the lubrication approximation is a parabolic profile across the disk. In Sec. VII, we calculate higher order terms in an asymptotic expansion for small gravity and smaller, but nonzero, surface tension. For the remainder of this section we explore the consequences of the simple *ad hoc* assumption that the variation across the circles is parabolic, an assumption which fits the experimental data reasonably well.

Consider the circle which passes through $y=0$ and $x=-b$ on which $h=H(b)$. The center of the circle will be at $[-\gamma H^2(b),0]$ and its radius $b-\gamma H^2(b)$. Our *ad hoc* assumption of a quadratic profile is that

$$H(b) = H_m \frac{(1-b)(1+b-2b_m)}{(1-b_m)^2} \quad \text{in } b_m \le b \le 1, \tag{4}$$

where $b=1$ is the periphery of the disk and $b=b_m$ is the innermost circle of zero radius, i.e., $b_m=\gamma H^2(b_m)$. Applying the volume normalization to the circles,

$$\int_0^{H_m} [b - \gamma H^2(b)]^2 dH = 1,$$

we find that the maximum thickness H_m varies with the strength of gravity γ according to

$$\frac{\gamma^2}{210} H_m^5 + \frac{\gamma}{35} H_m^3 + \frac{1}{2} H_m = 1.$$

There is one real root which decreases slowly from $H_m=2$ at $\gamma=0$. By $\gamma=0.2844$, the center of the innermost circle reaches the periphery of the disk ($b_m \to 1$), i.e., all the circular characteristics touch the boundary at $(-1,0)$. Our simple *ad hoc* model therefore fails at $\gamma=0.2844$. Note that this value is very near the $\gamma \approx 0.30$ found for the maximum load in the experiments.

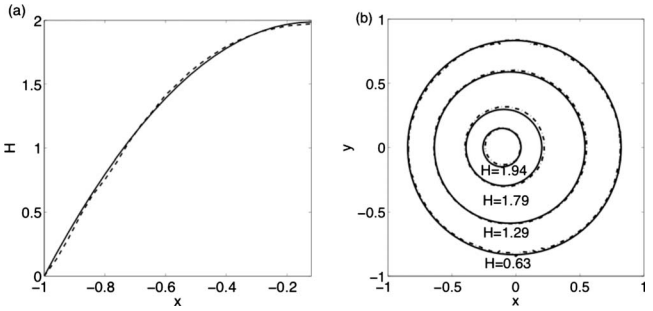

FIG. 7. For $\gamma=0.029$, (a) comparison of the *ad hoc* quadratic profile $H(b)$ of Eq. (4) (solid curve) with the profile obtained by solving Eq. (1) numerically (dashed curve) and (b) comparison of the thickness contour (3) with the *ad hoc* quadratic profile (4) (solid curve) and the numerically obtained contours (dashed curve).

Figure 7(a) compares the quadratic $H(b)$ of Eq. (4) with numerical predictions for $\gamma=0.029$. The quadratic profile agrees well with the numerically determined profile although the location of maximum thickness, $x=-b_{\max}$, differs slightly. Figure 7(b) shows that the contours predicted by Eqs. (3) and (4) are also in good agreement with the numerical results. This shows that the assumption of a quadratic thickness profile for $H(b)$ captures the essential features of the profile for small γ (<0.05). However, the quadratic profile (4) deviates from that predicted numerically for larger values.

VII. ASYMPTOTIC SOLUTION

For the detailed calculations of this section we adopted polar coordinates r,θ. For small gravity and even smaller, but nonzero, surface tension, as in the experiments, $\alpha \ll \gamma \ll 1$, we pose an asymptotic expansion

$$h(r,\theta;\gamma,\alpha) \sim h_0(r,\theta) + \gamma h_1(r,\theta) + \gamma^2 h_2(r,\theta) + \gamma^3 h_3(r,\theta) + \alpha[h_{10}(r,\theta) + \gamma h_{11}(r,\theta) + \gamma^2 h_{12}(r,\theta)]. \tag{5}$$

[In fact, no restriction need to be placed on the relative sizes of α and γ when studying the steady state, unlike the transients.[13]] Substituting into the governing Eq. (1) generates the following sequence of problems: At

$$O(\gamma^0): \frac{\partial h_0}{\partial \theta} = 0,$$

and so

$$h_0 = H_0(r).$$

At

$$O(\gamma^1): \frac{\partial h_1}{\partial \theta} = -H_0^2 \frac{dH_0}{dr} \sin\theta,$$

which gives

$$h_1 = H_0^2 \frac{dH_0}{dr} \cos\theta.$$

At

$$O(\gamma^2): \frac{\partial h_2}{\partial \theta} = -\frac{1}{r}\frac{\partial}{\partial r}\left(r H_0^4 \frac{dH_0}{dr} \sin\theta \cos\theta \right) - \frac{1}{r}\frac{\partial}{\partial \theta}\left(H_0^4 \frac{dH_0}{dr} \cos^2\theta \right),$$

which gives

$$h_2 = r\frac{d}{dr}\left(\frac{H_0^4}{r}\frac{dH_0}{dr} \right)\frac{1}{4}\cos 2\theta + f_2(r).$$

At

$$O(\gamma^3): \frac{\partial h_3}{\partial \theta} = -\frac{1}{r}\frac{\partial}{\partial r}[r(H_0^2 h_2 + H_0 h_1^2)]\sin\theta - \frac{1}{r}\frac{\partial}{\partial \theta}[(H_0^2 h_2 + H_0 h_1^2)\cos\theta].$$

Note that the constants of integration obtained on integrating with respect to θ at odd powers of γ are set to zero since otherwise changing the direction of rotation would change the sign of the term. The volume normalization requires

$$\int_0^1 H_0(r) r dr = \frac{1}{2} \quad \text{and} \quad \int_0^1 f_2(r) r dr = 0.$$

At this stage surface tension has not entered the calculation, and as a result we have two undetermined functions $H_0(r)$ and $f_2(r)$. The surface tension enters multiplied by the curvature, which we expand

$$\kappa \sim \kappa_0 + \gamma\kappa_1 + \gamma^2\kappa_2.$$

The leading order curvature is

$$\kappa_0 = \frac{1}{r}\frac{d}{dr}\left(r\frac{dH_0}{dr} \right)$$

and this forces the first surface tension correction at $O(\alpha^1)$,

$$\frac{\partial h_{10}}{\partial \theta} = -\frac{1}{r}\frac{\partial}{\partial r}\left(r\frac{H_0^3}{3}\frac{\partial \kappa_0}{\partial r} \right).$$

Since the right hand side is only a function of r and the solution for h_{10} must be periodic in θ, we conclude

$$h_{10} = 0 \quad \text{and} \quad r\frac{H_0^3}{3}\frac{\partial \kappa_0}{\partial r} = \text{const}.$$

Now the no-flux boundary condition at the edge of the disk gives that this constant must vanish, and so the curvature κ_0 must be constant. Applying the volume normalization, we have

$$H_0 = 2(1 - r^2).$$

This is the lubrication approximation to the spherical cap at zero gravity mentioned in Sec. VI.

From the above $H_0(r)$ we can evaluate the first gravity correction

$$h_1 = -16r(1 - r^2)^2 \cos\theta.$$

The first effect of gravity is therefore to move the maximum thickness of the film horizontally from the center of the disk to the upward moving side. The term gives the correction to the curvature

$$\kappa_1 = -128(-2r + 3r^3)\cos\theta,$$

which we need to find h_{11}, the first change in the surface due to surface tension. At

$$O(\gamma\alpha): \quad \frac{\partial h_{11}}{\partial \theta} = \frac{1}{r}\frac{\partial}{\partial r}\left(r\frac{H_0^3}{3}\frac{\partial \kappa_1}{\partial r} \right) + \frac{H_0^3}{3r^2}\frac{\partial^2 \kappa_1}{\partial \theta^2}.$$

Hence

$$h_{11} = 2048r(1 - r^2)^2(6 - 13r^2)\sin\theta.$$

This term moves the maximum thickness of the film vertically up.

The function $f_2(r)$ in the second gravity correction term h_2 is determined by the secularity condition in the problem for the surface tension term h_{12}. At

$$O(\gamma^2\alpha): \quad \frac{\partial h_{12}}{\partial \theta} = \frac{1}{r}\frac{\partial}{\partial r} r q_r + \frac{1}{r}\frac{\partial}{\partial \theta} q_\theta,$$

where

$$q_r = -H_0^2 h_{11} \sin\theta + H_0^2 h_1 \frac{\partial \kappa_1}{\partial r} + \frac{H_0^3}{3}\frac{\partial \kappa_2}{\partial r}.$$

For h_{12} to be periodic, we need the θ-average of the non-θ-derivative term to vanish, i.e.,

$$\left\langle \frac{1}{r}\frac{\partial}{\partial r} r q_r \right\rangle = 0,$$

where the angled brackets denote an average over θ. Hence $\langle r q_r \rangle$ must be constant, independent of r. By the no-flux boundary condition, this constant must vanish. Hence

$$\left\langle \frac{H_0^3}{3}\frac{\partial \kappa_2}{\partial r} \right\rangle = \langle H_0^2 h_{11} \sin\theta \rangle - \left\langle H_0^2 h_1 \frac{\partial \kappa_1}{\partial r} \right\rangle.$$

Substituting all our results above, we find the equation

$$\frac{d}{dr}\left[\frac{1}{r}\frac{d}{dr}\left(r\frac{df_2}{dr} \right) \right] = -6144r(1 - r^2)^2.$$

The solution satisfying the boundary condition $f_2(1) = 0$ and the volume normalization is

$$f_2 = \tfrac{16}{15}(1 - r^2)(-29 + 115r^2 - 65r^4 + 15r^6).$$

Finally, we can now evaluate the second and third corrections due to gravity

$$h_2 = 128r^2(1 - r^2)^3 \cos 2\theta + f_2(r),$$

$$h_3 = -5120r^3(1 - r^2)^4\cos^3\theta + \frac{256r}{15} \times (41 + 185r^2 - 595r^4 + 315r^6)(1 - r^2)^2\cos\theta.$$

We have now evaluated all the terms in the asymptotic ex-

pansion (5), except for the second surface tension correction h_{12}.

It can be checked that our asymptotic solution is constant on suitably offset characteristic circles if surface tension is set to zero, $\alpha=0$. The asymptotic solution fails to have the quadratic profile of our simple *ad hoc* model at $O(\gamma)$. Moreover, while the asymptotic solution has a maximum of the thickness of the film which increases slowly as $2+\frac{16}{15}\gamma^2$, the *ad hoc* model has a maximum which decreases as $2-\frac{16}{35}\gamma$.

The asymptotic solution to $O(\gamma^3, \alpha\gamma)$ is plotted with dashed curves in Figs. 3–5. The asymptotic solution is in good agreement with the measurements and numerical solution for $\gamma=0.029$ and 0.058. For the larger value $\gamma=0.116$, there are deviations which appear unphysical. More terms in the expansion are clearly needed for $\gamma>0.1$.

ACKNOWLEDGMENTS

The work described in this paper was supported by the Indian Institute of Technology Bombay Startup under Grant No. 03IR032. We also thank Professor D. V. Khakhar, Professor N. B. Ballal, and G. R. Shevare for useful discussions. N.H.P. acknowledges IIT Bombay for the Ph.D. fellowship.

[1] A. Oron, S. H. Davis, and S. G. Bankoff, "Long-scale evolution of thin liquid film," Rev. Mod. Phys. **69**, 931 (1997).
[2] L. Landau and B. Levich, "Dragging of a liquid by a moving plate," Acta Physicochim. URSS **17**, 42 (1942).
[3] H. K. Moffatt, "Behavior of a viscous film on the outer surface of a rotating cylinder," J. Mec. **16**, 651 (1977).
[4] M. Zanfir, X. Sun, and A. Gavriilidis, "Investigation of a rotating disc reactor for acetone stripping and asymmetric transfer hydrogenation: Modelling and Experiments," Chem. Eng. Sci. **62**, 741 (2007).
[5] A. Friedman, L. Robbins, and R. Woods, "Effect of disc rotational speed on biological contactors efficiency," J. Water Pollut. Control Fed. **51**, 2678 (1979).
[6] N. Hamill, L. Weatherley, and C. Hardacre, "Use of a batch rotating photocatalytic contactor for the degradation of organic pollutants in waste water," Appl. Catal., B **30**, 49 (2001).
[7] A. Sakurai, H. Imai, Y. Takenaka, and M. Sakaribara, "Simulation of citric acid production by rotating disc contactor," Biotechnol. Bioeng. **56**, 689 (1997).
[8] B. Woo, K. Choi, and K. Song, "Melt polycondensation of bisphenol A polycarbonate by forced gas sweeping process II. Continous rotating disc reactor," Ind. Eng. Chem. Res. **40**, 3459 (2001).
[9] A. G. Emslie, F. T. Borron, and L. G. Peck, "Flow of a viscous liquid on a rotating disc," J. Appl. Phys. **29**, 858 (1958).
[10] N. Fraysse and G. M. Homsy, "An experimental study of rivulet instabilities in centrifugal spin coating of viscous Newtonian and non-Newtonian liquids," Phys. Fluids **6**, 1491 (1994).
[11] S. K. Wilson, R. Hunt, and B. R. Duffy, "The rate of spreading in spin coating," J. Mech. **413**, 65 (2000).
[12] T. G. Myers and J. P. Charpin, "The effect of the Coriolis force on axisymmetric rotating thin film flows," Int. J. Non-linear Mech. **36**, 629 (2001).
[13] E. J. Hinch, M. A. Kelmanson, and P. D. Metcalfe, "Shock-like free-surface perturbations in low-surface-tension, viscous, thin-film flow exterior to a rotating cylinder," Proc. R. Soc. London, Ser. A **460**, 2975 (2004).